Progress In Electromagnetics Research C, Vol. 104, 85–97, 2020

Impact of Users' Finger on the Amount and Direction of Radiated Power from a 28 GHz 4-Element MIMO Antenna Mobile Terminal

Ahmed M. Elshirkasi[1], Azremi Abdullah Al-Hadi[1, *], Ping Jack Soh[1], Mohd Fais Mansor[2], Rizwan Khan[3], and Prayoot Akkaraekthalin[4]

Abstract—This paper investigates the effect of index finger position and distance on the radiated power of 4-element MIMO antenna, operating at 28 GHz. The antenna elements (AEs) are located at the top corner of the user terminal and separated at a distance of half a wavelength. Four different finger placements were investigated, one placement over each AE with six interaction distances between the AEs and the finger at each position starting from 0 up to 2.5 mm. When the finger is placed on an edge AE, the other edge AE maintained above 85% of its free space radiated power irrespective of the interaction distance. However, the radiated power of each AE was severely affected when the finger was placed on it or on the AE adjacent to it. This effect ranged from total blockage at direct interaction with the element (with a distance of 0 mm) to maintaining more than around 60% of free space radiated power after the interaction distance is increased to more than 2.0 mm. Besides the effects of the index finger on the amount of radiated power, this work also investigated the direction of radiated power resulting from the influence of this finger.

1. INTRODUCTION

The fifth-generation (5G) mobile communication networks aim to support massive number of devices with higher capacity, data rate, less latency, improved spectral energy, and cost considerations [1, 2]. However, the sub-6 GHz frequency bands in mobile communication systems are insufficient to meet the increasing data rate demand in the upcoming 5G communication system [3]. Therefore, investigating frequency bands in the millimeter range is one of the solutions and has intensified in recent years, both in the industrial and academic research fields [4–7]. Different millimeter bands were proposed during the World Radio Conference in 2015 (WRC-15) for 5G mobile communication systems, i.e., from 24.25 to 27.5 GHz, 31.8 to 33.4 GHz, 37 to 43.5 GHz, 45.5 to 50.2 GHz, 50.4 to 52.6 GHz, 66 to 76 GHz, and 81 to 86 GHz [8–10]. However, millimeter-wave signals are expected to experience much higher path losses than sub-6 GHz waves, potentially resulting in significant reduction of the link's signal-to-interference-plus-noise ratio [11, 12]. Thus, beamforming is proposed as one of the solutions to alleviate the problem of path loss, and this technique is proposed to be applied at both ends of the link of the base station and mobile terminal [13]. Phased arrays on the mobile terminal are used to steer the beam, and they can provide gain up to 10 dBi and are therefore an efficient solution to compensate the high path loss when operating at millimeter waves [14, 15].

Received 1 June 2020, Accepted 9 July 2020, Scheduled 30 July 2020

* Corresponding author: Azremi Abdullah Al-Hadi (azremi.abdullah@gmail.com).

[1] Advanced Communication Engineering (ACE) Center of Excellence, School of Computer and Communication Engineering, Universiti Malaysia Perlis, Kangar, Perlis 01000, Malaysia. [2] Centre of Advanced Electronic and Communication Engineering, Faculty of Engineering and Built Environment, Universiti Kebangsaan Malaysia, UKM Bangi, Selangor 43600, Malaysia. [3] Department of Research and Development, Laird Technologies (M) Sdn Bhd, Penang, Malaysia. [4] Department of Electrical and Computer Engineering, Faculty of Engineering, King Mongkut's University of Technology North Bangkok (KMUTNB), 1518 Pracharat 1 Rd., Wongsawang, Bangsue, Bangkok 10800, Thailand.

On the other hand, due to the short wavelength in millimeter bands, MIMO antennas on the user terminal can be closely packed in small areas on the mobile terminal with high performance [16, 17]. However, millimeter-wave signals are very sensitive to physical blockage by the user's body [18–20]. The energy of the wireless signals at 15 GHz can penetrate less than 2 mm into the body tissues, and this penetration distance is reduced by half at 30 GHz [21]. Moreover, direct blockage of the antenna elements by the user's body in mm-wave bands may cause link losses up to 30 dB [22]. Thus, the performance of MIMO antennas on mobile terminal needs to be investigated under the influence of human body effects, so that solutions can be proposed to mitigate this impact and to improve the performance.

Many researchers have investigated the human body effects on millimeter-wave MIMO antennas on mobile terminal from different perspectives. For examples, an analytical study has been conducted in [23] to explore the impact of the human body on the propagation of millimeter-waves. In [24], the effects of the user's body on a 10-element MIMO antenna from a Sony mobile terminal prototype operating at 28 GHz has been statistically studied using measurements from twelve volunteers in an anechoic chamber, and the mobile terminal was evaluated both in data and talk modes. On the other hand, two other studies reported results from real human body measurements inside anechoic chambers for phased arrays working at 15 GHz [19] and 28 GHz [25], and radiation patterns of the mobile terminal operating in talk and data modes were analyzed using different metrics such as coverage efficiency and probability of detection. Meanwhile, a different approach to study user's body impact on millimeter-wave MIMO antenna has been presented in [26] and [27]. The effects of hand blockage on 5G millimeter MIMO antenna in a mobile terminal were studied by using the combination of different handgrips and different antenna placements using a beamforming codebook, and the aim of these two studies is to find the optimal combination of antenna elements placement on the chassis and beamforming codebook. Next in [28], the radiation performance of a 10-element MIMO antenna operating at 28 GHz was studied. The effect of the fingertip was investigated on a one antenna terminal element only. Two positions of the fingertip were considered; when the fingertip is positioned directly on the element and when the fingertip is 10 mm away from the same terminal element. Despite that, this research did not study the effects of the fingertip on other elements with 0 and 10 mm distances, and did not consider the effects when the finger is placed over other adjacent elements. Moreover, the interaction distance between the fingertip and antenna elements was also not investigated. On the contrary, the work in [29] experimentally studied the effect of the finger on the matching and beamforming ability of a four-element MIMO antenna operating at 26 GHz. Despite these interesting features, the effect of the antenna when placed at different distances from the finger was not investigated in detail.

In this work, the effects of the user's hand grip, particularly the index finger, are investigated via simulations at 28 GHz in terms of radiated power and direction of radiation from a four-element MIMO antenna. The user's index finger is positioned on the top of each antenna element (AE) and is studied by assessing the radiated power of all AEs, including those in its vicinity. Besides that, this study also includes the effects of six different distances (d) between the finger and AEs when being positioned over a specific AE. It is worth mentioning that there are a total of 29 simulated scenarios in this research, which include cases with and without casing in free space, and with the index finger considered. Moreover, the index finger used in this work is a custom-designed model which is yet to be available in any standard human hand phantoms.

2. MIMO ANTENNA DESIGN AND FINGER MODEL

The MIMO antenna used in this paper is based on the design in [30] which is a planar four-element MIMO antenna operating at 28 GHz. In this design, a four-element MIMO antenna is placed on the top right corner of the chassis, and the AEs are separated from each other by half a wavelength. Two operating cases are considered; when the mobile terminal is assessed in free space and when the user's index finger is placed on top of four different antenna elements located at different positions P1, P2, P3, and P4. At each position, investigation was performed with six different distances (d) between the finger and the AE, i.e., 0.0, 0.5, 1.0, 1.5, 2.0, and 2.5 mm. In wavelength (λ) at 28 GHz, the value of d is 0λ, 0.05λ, 0.09λ, 0.14λ, 0.19λ, 0.23λ, respectively. The $d = 0$ mm spacing is impractical due to the existence of the casing between antenna and index finger in real devices. However, this was considered

Table 1. Dimensions and material properties of the substrate, AEs and finger phantom.

Chassis substrate	Dimensions: $110 \times 55 \times 0.13\,\text{mm}^3$
	Relative permittivity: $\varepsilon_r = 3$
	Loss tangent: 0.0013
Antenna elements (AEs)	Slotted area of each AE: $2.2 \times 5.3\,\text{mm}^2$
	Separation distance between adjacent AEs: $\frac{\lambda}{2} = 5.35\,\text{mm}$
	Feeding mechanism: $50\,\Omega$ transmission line
Finger phantom model	Dimensions: $78 \times 17 \times 12\,\text{mm}^3$
	Tissue relative permittivity: $\varepsilon_r = 3$
	Tissue conductivity: $\rho = 31.91\,\text{S/m}$

in this research as the hypothetical worst case scenario. A casing was then added over the antenna, and the radiated power was investigated in free space and when finger index is placed at position P1. Unlike in sub-6 GHz frequency bands where standard CTIA body parts (hand and head) are available for simulations and measurements, there is yet to be any standard phantoms available for use in the frequency bands above 10 GHz [11]. Therefore, a custom-designed finger with dimensions and material properties is introduced in this work for use in simulations, as listed in Table 1. In addition to that, the values of finger tissue properties are obtained from [23]. Besides the finger, the dimensions and material properties of the chassis and AEs are also summarized in this table. A major challenge when studying the user's body effects in the mm-wave range is the resource-intensive and time-consuming simulations due to the short wavelengths. To optimize this in practice while maintaining satisfactory accuracy, the full hand grip is truncated to consider only the fingertip modeled in proximity of the mobile terminal.

Figure 1(a) shows the detailed geometry of the MIMO antenna, whereas the four finger positions are illustrated in Figure 1(b). To investigate the performance with casing, the antenna is confined to a bounding box dimensioned at $115 \times 60 \times 5\,\text{mm}^3$. The thickness of the casing is 1 mm, modeled using a material with $\varepsilon_r = 3.5$ [28], as shown in Figures 1(c) and (d). For a fair comparison and to emulate the worst case interaction, the antenna was positioned within the box so that a minimal separation to the

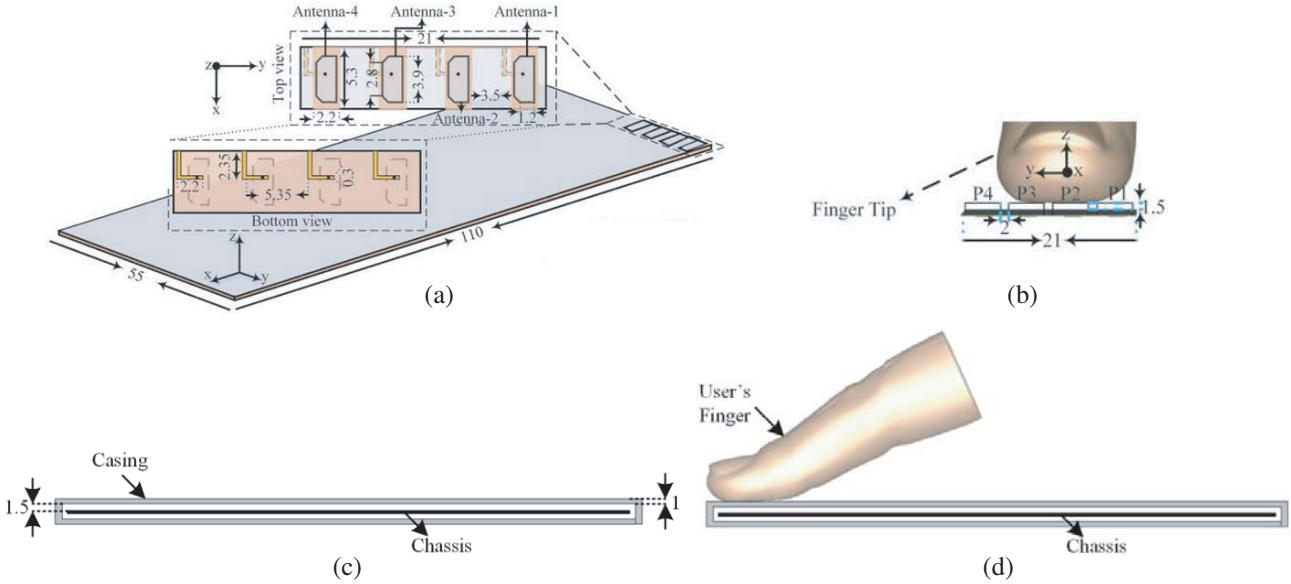

Figure 1. (a) Detailed geometry of the chassis and AEs [30]. (b) Positions of the finger over the AEs [30]. (c) Dimensions of the casing. (d) Finger index placed with casing.

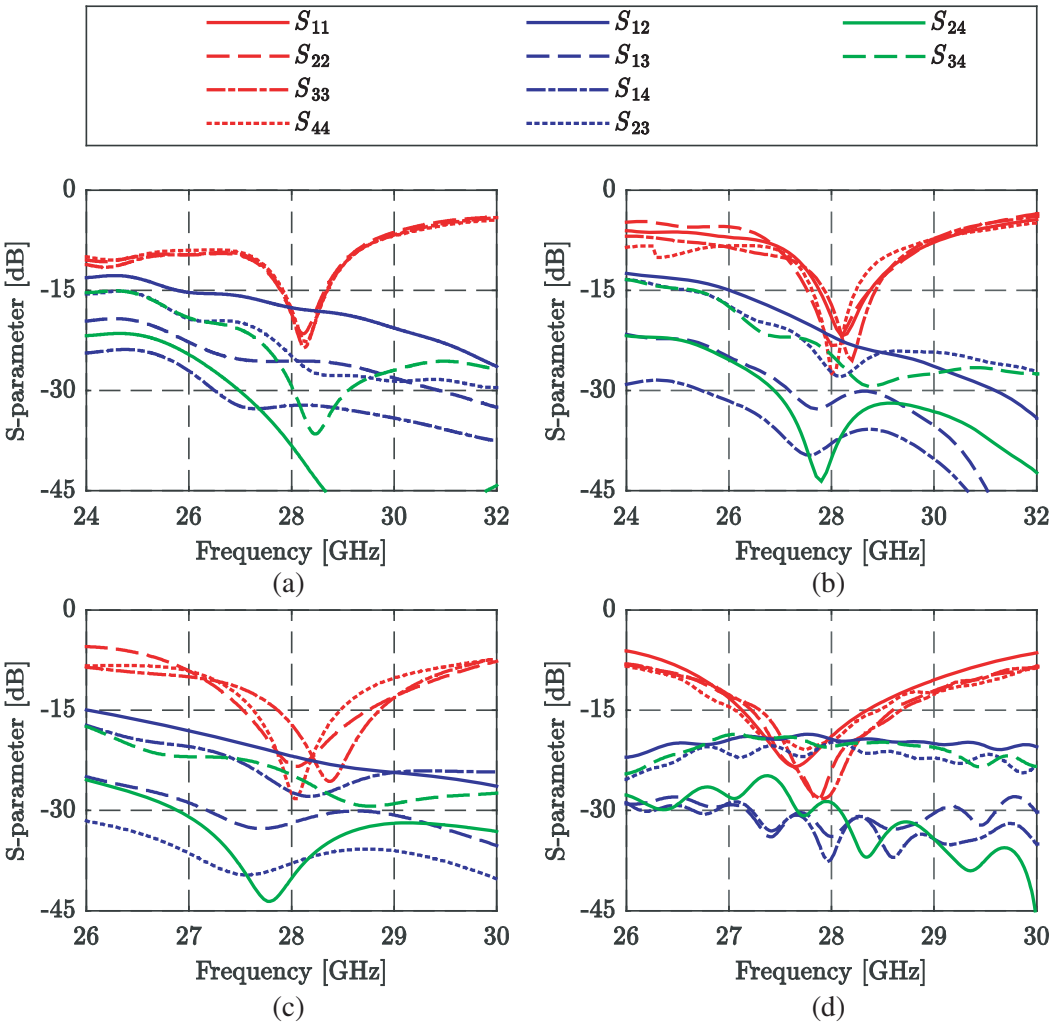

Figure 2. S-parameters of AE1: (a) In free space without casing [30]. (b) With finger located at P1 and $d = 2.5$ mm and without casing [30]. (c) Free space with casing. (d) With finger located at P1 and with casing.

user finger was achieved. The resulting S-parameters with and without the casing in free spacing and with the index finger located at P1 are shown in Figure 2.

3. RADIATED POWER RESULTS AND DISCUSSION

This work assesses the radiated power from the AEs as the main performance metric. The radiated power (P_r) of the antenna is calculated as follows [31]:

$$P_r = \int_0^{2\pi} \int_0^{\pi} U \sin(\theta)\, d\theta d\phi \tag{1}$$

where U is the radiation intensity of the antenna calculated from the far-field radiation pattern data as follows:

$$U = \frac{1}{2\eta_0} \left(|E_\theta|^2 + |E_\phi|^2 \right) \tag{2}$$

where η_0 is the free space intrinsic impedance, and E_θ and E_ϕ are the electric fields in the vertical and horizontal polarization, respectively. However, the radiation pattern of an antenna is either simulated or measured at discrete elevation and azimuth directions, i.e., $[\theta_0,\theta_1,\ldots\theta_{N-1}]$ and $[\phi_0,\phi_1,\ldots\phi_{M-1}]$. The radiated power P_r can then be calculated numerically from the discretized values in Equations (1) and (2) using:

$$P_r = \frac{1}{2\eta_0}\sum_{i=0}^{\theta_{N-1}}\sum_{j=0}^{\phi_{M-1}}\left(\left|E_\theta\left(\theta_i,\phi_j\right)\right|^2+\left|E_\phi\left(\theta_i,\phi_j\right)\right|^2\right)\sin\left(\theta_i\right)\cdot\Delta\theta\cdot\Delta\phi \tag{3}$$

where $\Delta\theta$ and $\Delta\phi$ are the simulation step sizes

Figure 3 shows the radiation intensity of AE1 in free space. In this figure, the radiation intensity from the AE is divided into 45° windows along the elevation direction. These windows will be used to study how the presence of the user finger affects the amount of radiated power in each window compared to free space. The radiated power in each window is calculated from Eq. (1) by replacing the overall limits of integration of the ϕ variable (i.e., from 0 to 2π) by the limits of the 45° window.

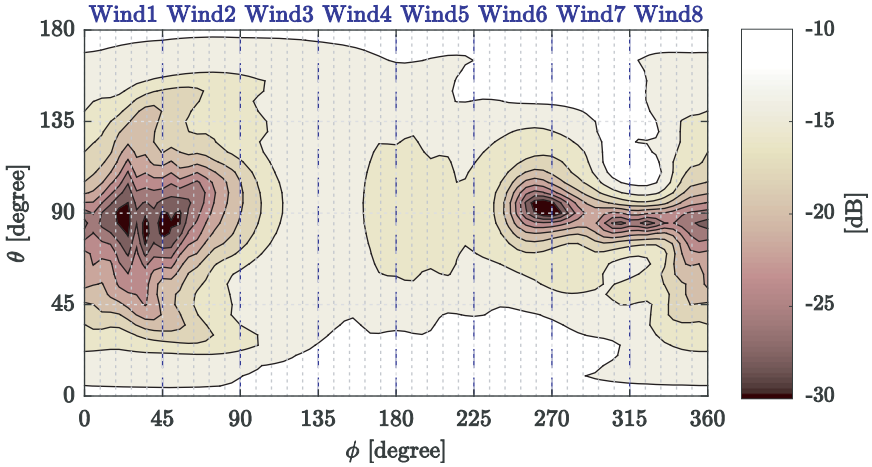

Figure 3. Radiation intensity of AE1 in free space and its division into the 45° windows for analysis.

The radiation intensity resulting from each AE accounting for the effects of the index finger is shown in Figures 4 and 5. Radiation intensity resulted in the highest radiated power from each AE when $d = 2.5$ mm which is illustrated in Figure 4. AE1 and AE2 radiated their highest power when the index finger is placed furthest from them, which is at P4. Similarly, AE3 and AE4 radiated their highest power when the finger is placed on their far side, at P1. On the contrary, the radiation intensity that leads to the least radiated power is shown in Figure 5, caused by the direct contact between AEs and the index finger ($d = 0$ mm). All AEs are severely blocked when the finger is placed directly over them, except for AE3 which radiates the least power when finger is placed next to it at P4.

Next, the amount of radiated power from each AE in free space and under the influence of the index finger is shown in Figure 6. All four positions and six distances are plotted separately for clarity.

It is observed that in free space the AEs have similar radiated power, with values of −3.38, −3.46, −3.42, and −3.41 dB for AE1, AE2, AE3, and AE4, respectively. However, the AEs radiate differently under the influence of the index finger, depending on the position and the distance. In general, each AE is severely affected when the finger is positioned over it, besides on the adjacent AE. More deterioration can be seen as the distances between the AE and index finger is decreased, with the worst case (of nearly complete blockage) at 0.0 mm. From the same figure, it is also seen that AE1 is severely affected by the finger in positions P1 and P2 with shorter d. At P1 the radiated power of AE1 increased from 16.82 dB when $d = 0.0$ mm to around −5.27 dB when $d = 2.5$ mm. Similar radiated power from AE1 with a small amount of improvement is noticed when the finger is positioned at P2. On the other hand, the radiated power of AE1 is much improved as the finger is positioned further over P3 and P4. The radiated power

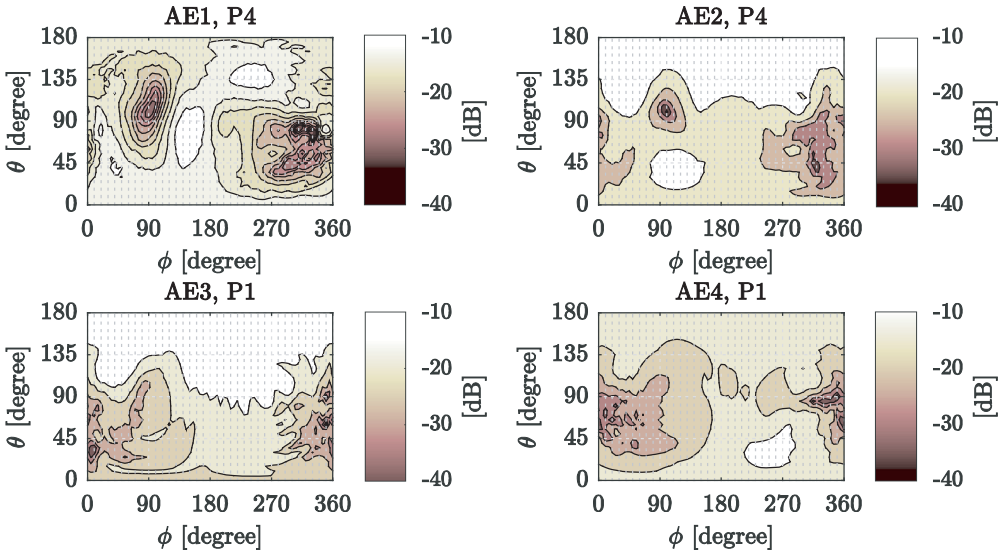

Figure 4. Radiation intensity from each AE which resulted in the highest radiated power in the presence of the index finger, with $d = 2.5$ mm.

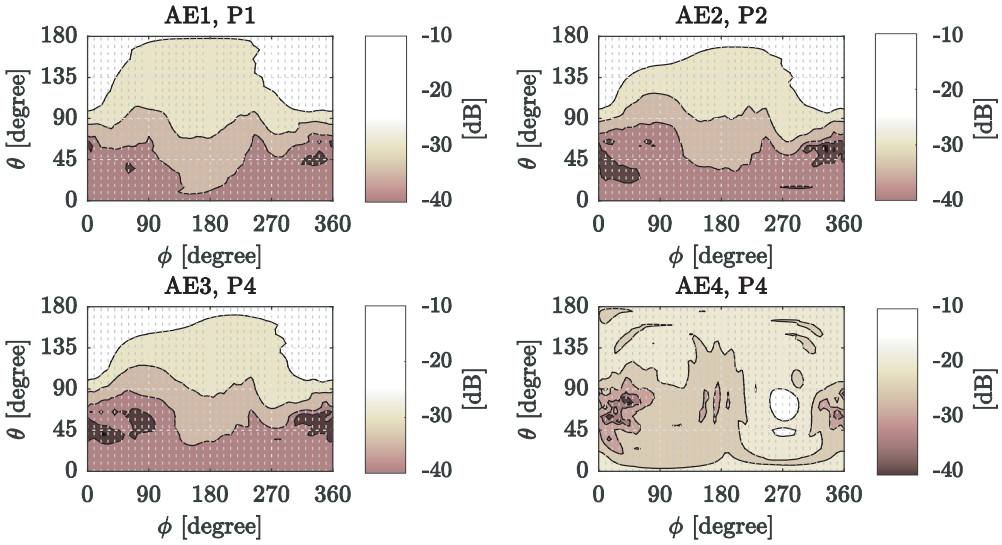

Figure 5. Radiation intensity from each AE that resulted in the least radiated power in the presence of an index finger with 0 mm distance.

from AE1 when the finger is positioned at P3 is gradually increased from −6.17 dB to −4.49 dB as d is increased from 0.0 to 2.5 mm. However, the radiated power of AE1 becomes independent of d when the finger is positioned at P4 with values around −3.91 dB. In general, it is also observed that AE2 is affected most significantly by the placement of the finger among the four AEs at all finger positions. When the finger is placed at P1, P2, and P3 with d of 0.0 mm, the radiated power of this element is less than −17.00 dB, with about 4.00 dB improvements when the finger is placed at P4. Performance of this element improved with an increasing d, with radiated power ranging from −5.65 dB to −4.71 dB (with $d = 2.5$ mm) when the finger is placed at P1 and P4, respectively. The next most affected element by the placement of the finger is AE3. This is especially obvious when the finger is located at P3 and P4. At $d = 0.0$ mm, the radiated power from AE3 is as low as −17.34 dB, −14.84 dB, −9.10 dB, and −6.56 dB at finger P4, P3, P2, and P1, respectively. On the other hand, these values increased to −5.63, −5.43, −4.96, and −4.71 dB with $d = 2.5$ mm when the same finger is positioned at P4, P3, P2, and

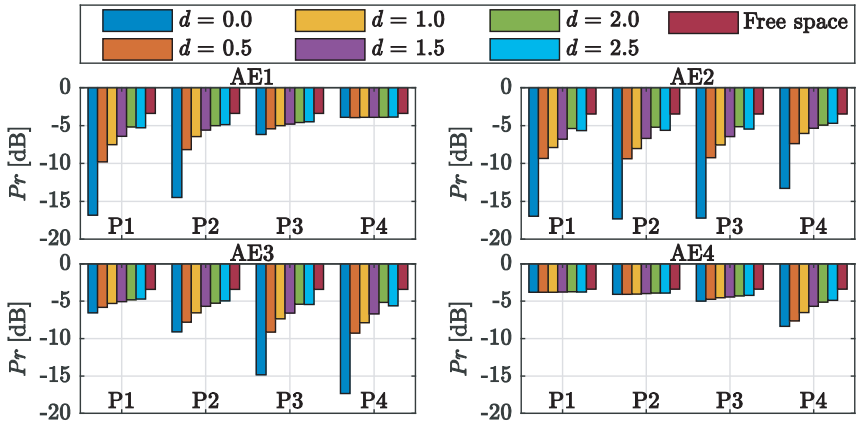

Figure 6. Amount of radiated power of different AEs with different finger positions and distances.

P1, respectively.

Finally, AE4 is the least affected element by the finger placement over the AEs. The radiated power from this element showed stable performance when the finger is located at P1, P2, and P3 with values of around −4 dB irrespective of d. However, the finger positioned at P4 relatively caused more degradation in radiated power. Its power ranged from −8.36 dB to −4.90 dB with an increasing d, from 0.0 to 2.5 mm, respectively.

Next, Figure 7 shows the radiated power efficiency (η_{P_r}) of the AEs at different finger positions and distances, with η_{P_r} defined in this work as:

$$\eta_{P_r} = \frac{P_{r\ tot,\ with\ finger}}{P_{r\ tot,\ free\ space}} \tag{4}$$

where $P_{r\ tot,\ with\ finger}$ and $P_{r\ tot,\ free\ space}$ are the total radiated powers under the influence of the finger and in free space, respectively.

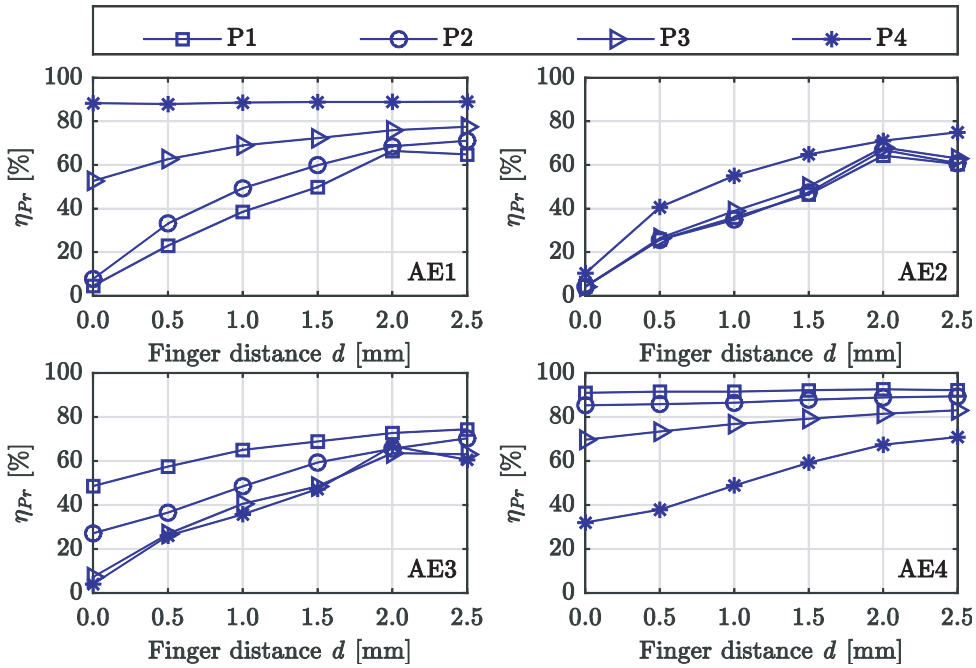

Figure 7. Radiated power efficiency η_{P_r} from each AE with different finger positions and distances.

Generally, it is observed that the antennas located at the edges (AE1 and AE4) maintained the highest radiated power efficiency under the influence of the finger. This is particularly evident when the finger is positioned over the furthest AE located on its opposite side. AE1 preserved around 88% of its free space radiated power efficiency when the finger is placed at P4, irrespective of the value of d. When varying the separation distance, the performance of AE1 degraded between 53% and 77% with an increasing d from 0.0 mm to 2.5 mm with the finger at P3. However, AE1 radiated only less than 7% compared to its free space power at P1 and P2 and $d = 0.0$ mm. Nonetheless, this radiated power efficiency improved with an increasing d about 70% at $d = 2.5$ mm.

Besides AE1, the other edge element (AE4) also exhibited higher radiated power efficiency. This element preserved above 91% and 85% of its free space radiated power when the finger is located at P1 and P2, irrespective of the value of d. However, less power is observed when the finger is placed at P3, with values between 69% and 83% at d of 0.0 mm and 2.5 mm, respectively. Besides that, this element is affected most when the finger is placed over it at P4 in direct contact (with $d = 0.0$ mm). In this case, AE4 radiated only 32% of its free space power. However, this efficiency improved with a larger d about 70% at d of 2.5 mm.

On the contrary, the AEs located in between AE1 and AE4 suffer from the highest radiated power loss under the influence of the user's finger in the same way. For instance, AE2 is severely blocked by the finger at distance $d = 0$ mm, and its radiated power efficiency is less than 10%, irrespective of the finger position. The radiated power of AE2 gradually improved as the finger is located over AEs located further away, with a maximum efficiency of around 75% at $d = 2.5$ mm in P4. This efficiency is degraded to about 65% at distance of 2.0 mm when the finger is located over the other three positions. Finally, the performance of AE3 is similar to AE2 in general, with slightly higher values. At $d = 0.0$ mm, this element radiates at 48% and 27% of its free space power when the finger is placed over P1 and P2. However, the radiation from this AE is significantly degraded when the finger is located at P3 and P4, with a radiated efficiency less than 7% in comparison to free space. Meanwhile, when placed in these

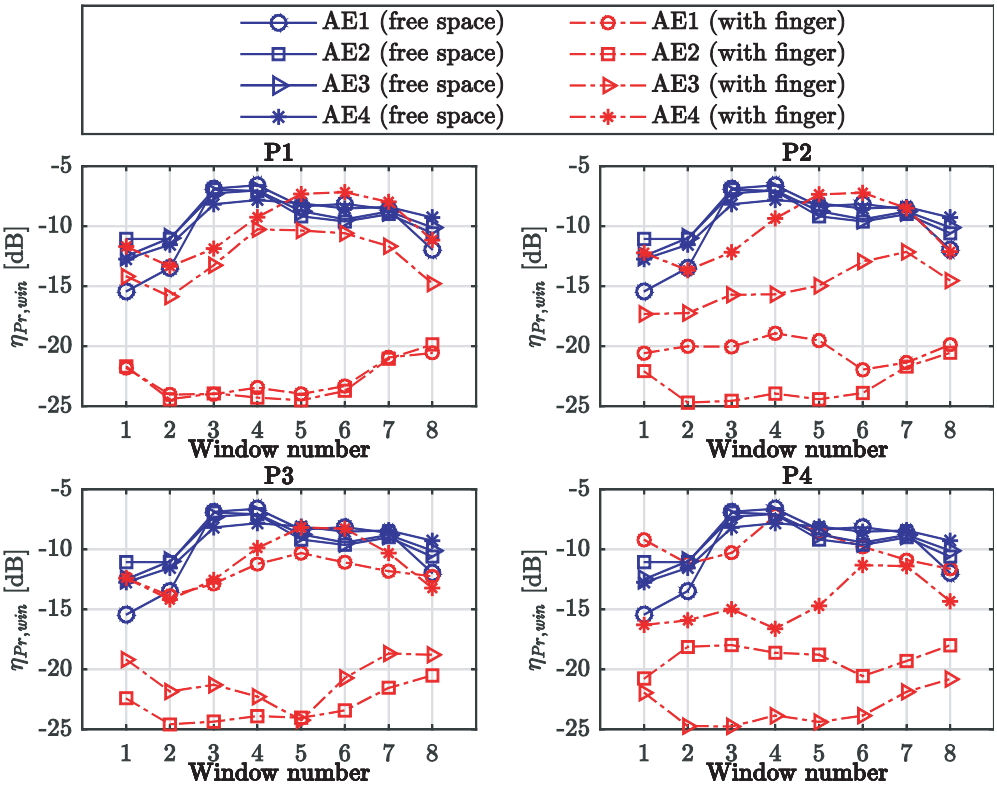

Figure 8. Window radiated power efficiency $\eta_{P_r,win}$ of different finger positions at $d = 0.0$ mm in free space (solid) and with finger (dashed).

locations, the performance in terms of radiation efficiency improved as d is increased, with a maximum of 74% at $d = 2.5$ mm (and finger located at P1).

It can also be summarized that the radiated power efficiency is heavily influenced by d, as illustrated in Figure 7. A d of around 2.0 mm is needed to guarantee that more than 60% of free space power radiated irrespective of the finger position.

Besides the consideration of power blockage, the existence of the finger in proximity of the antenna elements may potentially alter the amount of radiated power in specific directions. Despite being an expected occurrence, this should to be minimized, especially in phased array implementations. To study this, the same concept in Eq. (4) is used to analyze window radiated power efficiency ($\eta_{P_r,win}$). This is defined as the ratio of the radiated power in the windows illustrated in Figure 3 to the total free space radiated power as follows:

$$\eta_{P_r,\,win} = \frac{P_{r\ win}}{P_{r\ tot,\ free\ space}} \tag{5}$$

where $P_{r\ win}$ is the radiated power in the window in free space and under the influence of the finger, and $P_{r\ tot,\ free\ space}$ is the total radiated power in free space. Besides the amount of power, $\eta_{P_r,\,win}$ also indicates the directions in which the maximum power is radiated and how finger affects these directions.

Figure 8 and Figure 9 show the results of window radiated power efficiency $\eta_{P_r,\,win}$ with $d = 0.0$ and 2.5 mm, respectively. In both figures, the free space $\eta_{P_r,\,win}$ of the four AEs featured the same patterns, with the maximum radiated power directed towards the third and fourth windows, i.e., ϕ from 90° to 180°. In Figure 8 when $d = 0.0$ mm, the small amount of radiated power from the blocked AEs is distributed in many different directions. In this figure, the less affected AEs radiated a high portion of power with a shift towards two to three adjacent windows compared with their free space directions. Besides the improved radiated power amount in Figure 9 with $d = 2.5$ mm, it is clear that the AEs maximum power is radiated with shifts towards the right between 90° and 135° compared to the maximum free space radiated directions.

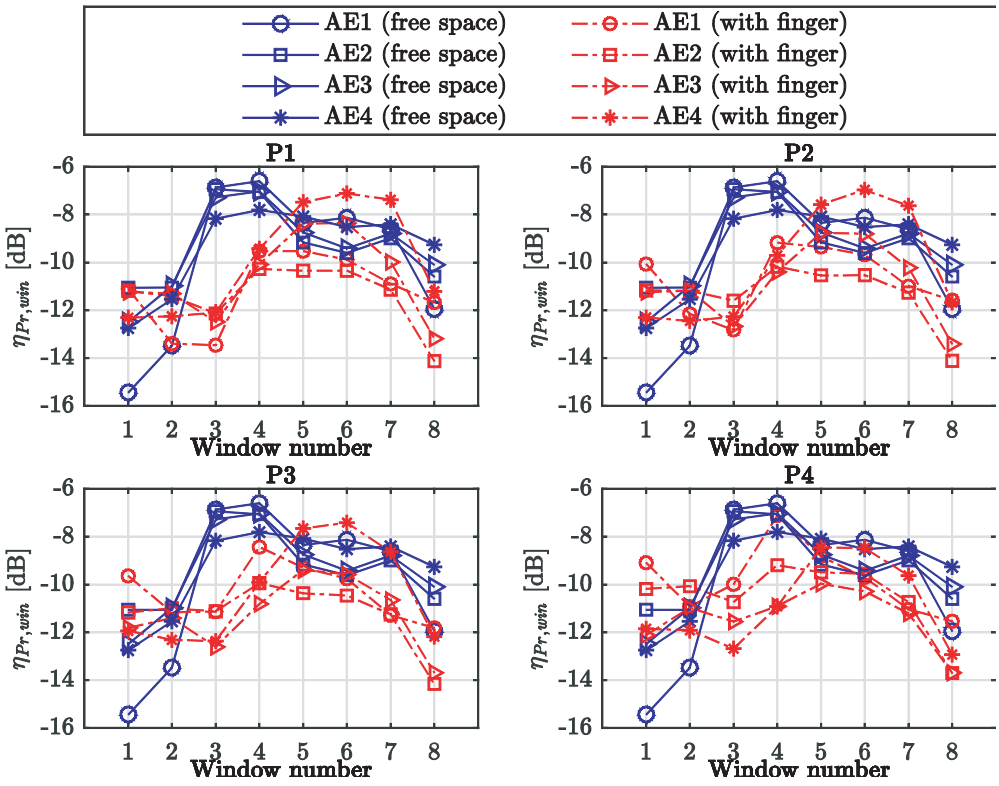

Figure 9. Window radiated power efficiency $\eta_{P_r,win}$ of different finger positions at d= 2.5 mm in free space (solid) and with finger (dashed).

The next part of this investigation aims to study the effect of the casing. This is performed by assessing the radiated power and radiation efficiency for the cases of with and without casing, both in free space and with the finger index located at position P1. As aforementioned, the combined thickness of the air gap and the casing is 2.5 mm, as illustrated in Figure 1(c). Thus to ensure a fair comparison, the gaps between the finger placed at P1 for the antenna with and without casing are both set at $d = 2.5$ mm. These results are presented in Figure 10. Comparison of both cases in free space and with the index finger indicated slightly higher radiated power with casing. More specifically, in free space with casing, all AEs radiated with about same level of power at -3.15 dB. This value is only approximately 0.20 dB higher than the radiated power in free space radiated power from the AEs without casing. This is due to the scattering of waves on the casing, as also reported in [29]. Such scattering causes more fluctuations in the fields, resulting in the slightly higher summed values from all

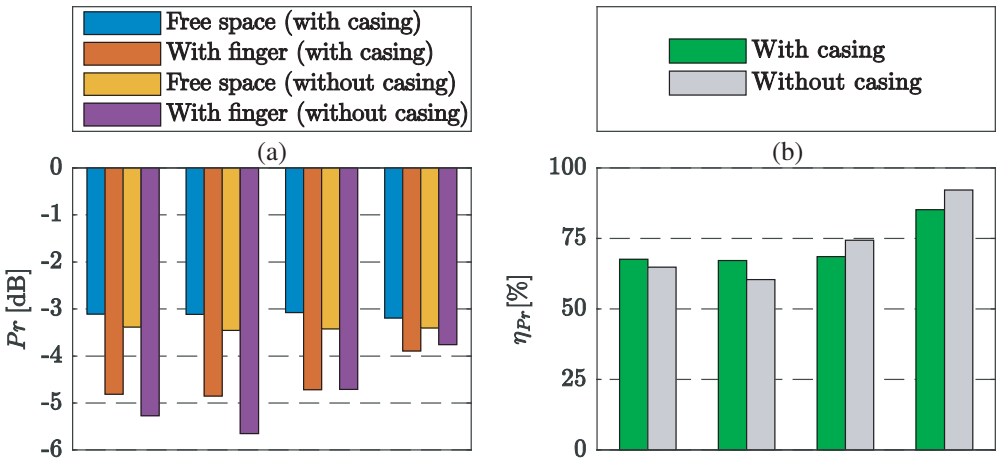

Figure 10. Performance of different AEs with and without casing in free space and with finger located at position P1 and $d = 2.5$ mm in terms of; (a) Radiated power, and (b) Radiation efficiency.

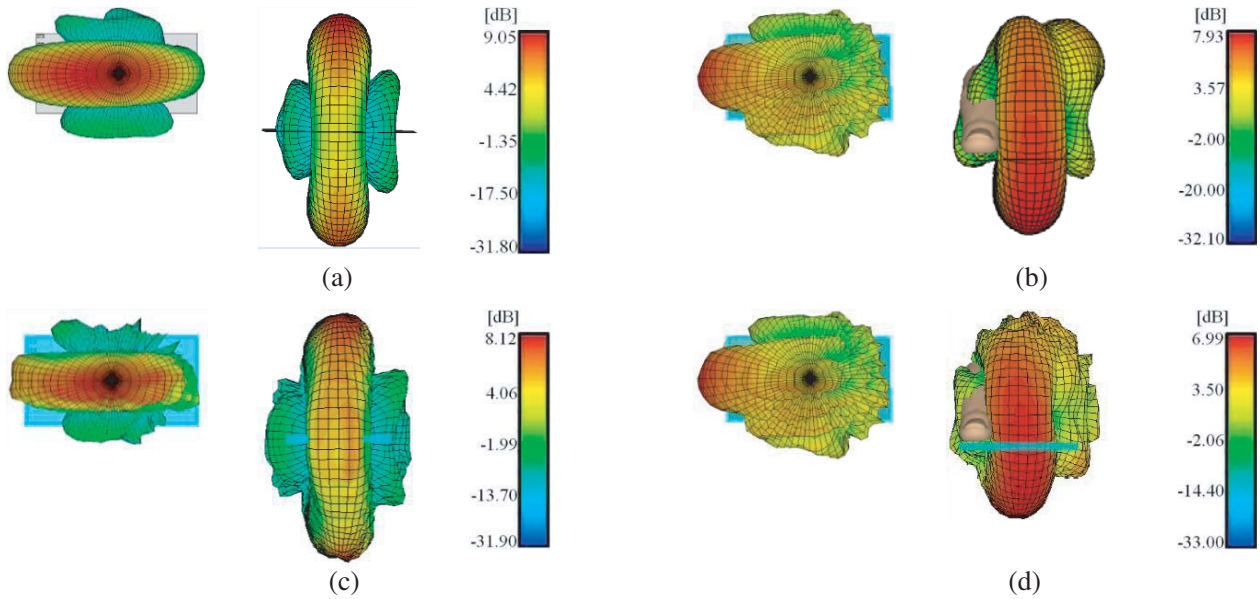

Figure 11. Combined gain of the MIMO antenna in xy plane (left) and yz plane (right) for; (a) Without casing in free space. (b) Without casing with finger at P1 and $d = 2.5$ mm. (c) With casing in free space. (d) With casing and finger.

components in Eq. (3). On the other hand, the radiated powers with finger for AE1, AE2, AE3, and AE4 are −4.81 dB, −4.81 dB, −4.72 dB, and −3.94 dB, respectively. This indicates that the element located furthest away for AE1 is least affected by the finger, which is the same observation with the antenna without casing. Meanwhile, the radiation efficiencies with and without casing indicated similarly, as shown in Figure 10(b). The radiation efficiencies of AE1 are 68% and 65% with and without casing, respectively, whereas the efficiency of AE2 improved from 60% without casing to 67% with casing. On the contrary, the radiation efficiencies of AE3 and AE4 degraded to 68% and 85%, respectively, when the casing is considered. This is a decrease of about 7% for both AEs in comparison to the values without casing.

Finally, the radiation pattern of the MIMO antenna is studied when all AEs are simultaneously excited. The previous scenarios with and without casing are repeated, this time, considering the index finger positioned at P1. This configuration is aimed at evaluating unlike any other cases in this work, where each antenna element is separately excited. The combined gain is shown in Figure 11.

The radiated power and radiated power efficiency are presented in Figures 12(a) and (b), respectively. The radiated power levels in free space are similar, with values of 2.32 dB (without casing) and 2.55 dB (with casing). The placement of the finger reduces these values to comparable levels of 0.55 dB and 0.60 dB for the cases of with and without casing, respectively. The radiated power efficiencies are also similar for both without and with casing, at 66% and 64%, respectively.

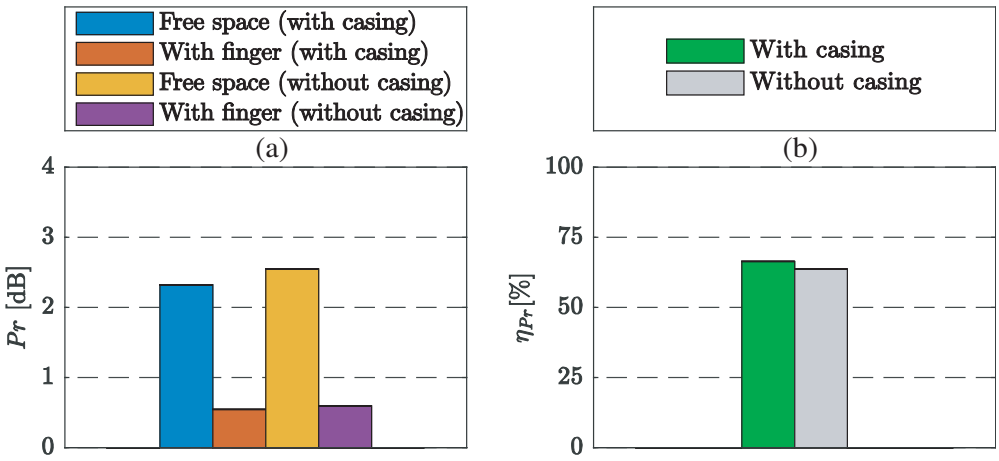

Figure 12. Combined radiation pattern performance (array performance) with and without casing in free space and with finger at position P1 and $d = 2.5$ mm in terms of; (a) Radiated power. (b) Radiation efficiency.

4. CONCLUSION

This work studied the amount and direction of radiated power from millimeter wave MIMO antennas located on a mobile terminal in free space and in the vicinity of a user's finger. Millimeter wave MIMO antenna elements can be designed in a compact area with satisfactory free space performance. However, upon the placement of a user's finger, the performance is significantly dependent on the separation distance between AEs and the distance between the finger and these AEs. Total blockage of the radiated power from the AE may occur, especially when the finger is placed directly onto the antenna element or onto the adjacent element. It is also found that the inter-element separation distance of $\lambda/2$ at 28 GHz (i.e., 5.35 mm) is insufficient to isolate the effects of the finger when it is placed on adjacent AEs. Thus, further investigation was conducted to study the required inter-element separation distance due to this effect. It is then found from this study that a minimum of 2 mm distance between the finger and antenna element is needed to achieve at least 60% of the amount of radiation in free space. This investigation also indicated that more separation is needed for more radiated power from the MIMO antennas and ultimately bounds the allowable thickness of mobile devices. Besides its amount, the

direction of radiated power is also affected by the finger. Results indicate that when the finger is placed at a distance of 2.5 mm from the AE, the adjacent AEs featured closer performance to free space with a direction-shift of between 90° and 135°. Thus, it can be concluded that MIMO antenna designed for millimeter-wave mobile terminals must sufficiently space their AEs to reduce the influence of the user's finger located over the adjacent AEs.

ACKNOWLEDGMENT

The author would like to acknowledge the support from the Fundamental Research Grant Scheme (FRGS) under a grant number of FRGS/1/2019/TK04/UNIMAP/02/21 from the Ministry of Education Malaysia, and Thailand Research Fund through the TRF Senior Research Scholar Program under Grant RTA 6080008.

REFERENCES

1. Gupta, A. and R. K. Jha, "A survey of 5G network: Architecture and emerging technologies," *IEEE Access*, Vol. 3, 1206–1232, 2015.
2. Kim, Y., et al., "Feasibility of mobile cellular communications at millimeter wave frequency," *IEEE J. Sel. Top. Signal Process.*, Vol. 10, No. 3, 589–599, 2016.
3. Wang, C.-X., et al., "Cellular architecture and key technologies for 5G wireless communication networks," *IEEE Commun. Mag.*, Vol. 52, No. 2, 122–130, 2014.
4. Rappaport, T. S., R. W. Heath Jr, R. C. Daniels, and J. N. Murdock, *Millimeter Wave Wireless Communications*, Pearson Education, 2014.
5. Dehos, C., J. L. González, A. De Domenico, D. Ktenas, and L. Dussopt, "Millimeter-wave access and backhauling: the solution to the exponential data traffic increase in 5G mobile communications systems?" *IEEE Commun. Mag.*, Vol. 52, No. 9, 88–95, 2014.
6. Giordani, M., M. Mezzavilla, and M. Zorzi, "Initial access in 5G mmWave cellular networks," *IEEE Commun. Mag.*, Vol. 54, No. 11, 40–47, 2016.
7. Almasi, M. A., H. Mehrpouyan, V. Vakilian, N. Behdad, and H. Jafarkhani, "A new reconfigurable antenna MIMO architecture for mmWave communication," *2018 IEEE International Conference on Communications (ICC)*, 1–7, 2018.
8. Marcus, M. J., "5G and IMT for 2020 and beyond [Spectrum Policy and Regulatory Issues]," *IEEE Wirel. Commun.*, Vol. 22, No. 4, 2–3, 2015.
9. Sun, S., T. S. Rappaport, M. Shafi, P. Tang, J. Zhang, and P. J. Smith, "Propagation models and performance evaluation for 5G millimeter-wave bands," *IEEE Trans. Veh. Technol.*, Vol. 67, No. 9, 8422–8439, 2018.
10. Samimi, M. K. and T. S. Rappaport, "3-D millimeter-wave statistical channel model for 5G wireless system design," *IEEE Trans. Microw. Theory Tech.*, Vol. 64, No. 7, 2207–2225, 2016.
11. Naqvi, A. H. and S. Lim, "Review of recent phased arrays for millimeter-wave wireless communication," *Sensors*, Vol. 18, No. 10, 3194, 2018.
12. Liu, J., A. Vosoogh, A. U. Zaman, and J. Yang, "Design and fabrication of a high-gain 60-GHz cavity-backed slot antenna array fed by inverted microstrip gap waveguide," *IEEE Trans. Antennas Propag.*, Vol. 65, No. 4, 2117–2122, 2017.
13. Roh, W., et al., "Millimeter-wave beamforming as an enabling technology for 5G cellular communications: Theoretical feasibility and prototype results," *IEEE Commun. Mag.*, Vol. 52, No. 2, 106–113, 2014.
14. Ojaroudiparchin, N., M. Shen, S. Zhang, and G. F. Pedersen, "A switchable 3-D-coverage-phased array antenna package for 5G mobile terminals," *IEEE Antennas Wirel. Propag. Lett.*, Vol. 15, 1747–1750, 2016.
15. Zhang, S., X. Chen, I. Syrytsin, and G. F. Pedersen, "A planar switchable 3-D-coverage phased array antenna and its user effects for 28-GHz mobile terminal applications," *IEEE Trans. Antennas Propag.*, Vol. 65, No. 12, 6413–6421, 2017.

16. Hussain, M. T., M. S. Sharawi, S. Podilchack, and Y. M. M. Antar, "Closely packed millimeter-wave MIMO antenna arrays with dielectric resonator elements," *2016 10th European Conference on Antennas and Propagation (EuCAP)*, 1–4, 2016.
17. Liu, D., X. Gu, C. W. Baks, and A. Valdes-Garcia, "Antenna-in-package design considerations for Ka-band 5G communication applications," *IEEE Trans. Antennas Propag.*, Vol. 65, No. 12, 6372–6379, 2017.
18. Niu, Y., Y. Li, D. Jin, L. Su, and A. V Vasilakos, "A survey of millimeter wave communications (mmWave) for 5G: opportunities and challenges," *Wirel. Networks*, Vol. 21, No. 8, 2657–2676, 2015.
19. Zhao, K., J. Helander, D. Sjöberg, S. He, T. Bolin, and Z. Ying, "User body effect on phased array in user equipment for the 5G mmWave communication system," *IEEE Antennas Wirel. Propag. Lett.*, Vol. 16, 864–867, 2017.
20. Raghavan, V., et al., "Statistical blockage modeling and robustness of beamforming in millimeter-wave systems," *IEEE Trans. Microw. Theory Tech.*, 2019.
21. Wu, T., T. S. Rappaport, and C. M. Collins, "Safe for generations to come: Considerations of safety for millimeter waves in wireless communications," *IEEE Microw. Mag.*, Vol. 16, No. 2, 65–84, 2015.
22. 3GPP T R 38.901, "Study on channel model for frequencies from 0.5 to 100 GHz," 2017.
23. Wu, T., T. S. Rappaport, and C. M. Collins, "The human body and millimeter-wave wireless communication systems: Interactions and implications," *2015 IEEE International Conference on Communications (ICC)*, 2423–2429, 2015.
24. Syrytsin, I., S. Zhang, G. Pedersen, K. Zhao, T. Bolin, and Z. Ying, "Statistical investigation of the user effects on mobile terminal antennas for 5G applications," *IEEE Trans. Antennas Propag.*, 2017.
25. Syrytsin, I., S. Zhang, and G. F. Pedersen, "User impact on phased and switch diversity arrays in 5G mobile terminals," *Ieee Access*, Vol. 6, 1616–1623, 2018.
26. Raghavan, V., M.-L. Chi, M. A. Tassoudji, O. H. Koymen, and J. Li, "Antenna placement and performance tradeoffs with hand blockage in millimeter wave systems," *IEEE Trans. Commun.*, Vol. 67, No. 4, 3082–3096, 2019.
27. Alammouri, A., J. Mo, B. L. Ng, J. C. Zhang, and J. G. Andrews, "Hand grip impact on 5G mm wave mobile devices," *IEEE Access*, Vol. 7, 60532–60544, 2019.
28. Xu, B., et al., "Radiation performance analysis of 28 GHz antennas integrated in 5G mobile terminal housing," *Ieee Access*, Vol. 6, 48088–48101, 2018.
29. Nguyen, T. Q. K., M. S. Miah, L. Lizzi, K. Haneda, and F. Ferrero, "Experimental evaluation of user's finger effects on a 5G terminal antenna array at 26 GHz," *IEEE Antennas Wirel. Propag. Lett.*, 2020.
30. Khan, R., A. A. Al-Hadi, and P. J. Soh, "Efficiency of millimeter wave mobile terminal antennas with the influence of users," *Progress In Electromagnetics Research*, Vol. 161, 113–123, 2018.
31. Gross, F., *Smart Antennas with Matlab: Principles and Applications in Wireless Communication*, McGraw Hill Professional, 2015.